

First closed-loop visible AO test results for the advanced adaptive secondary AO system for the Magellan Telescope: MagAO's performance and status

Laird M. Close^{1a}, Jared R. Males^a, Derek Kopon^a, Victor Gasho^a, Katherine B. Follette^a, Phil Hinz^a, Katie Morzinski^a, Alan Uomoto^b, Tyson Hare^b, Armando Riccardi^c, Simone Esposito^c, Alfio Puglisi^c, Enrico Pinna^c, Lorenzo Busoni^c, Carmelo Arcidiacono^c, Marco Xompero^c, Runa Briguglio^c, Fernando Quiros-Pacheco^c, Javier Argomedo^c

^aCAAO, Steward Observatory, University of Arizona, Tucson AZ 85721, USA;

^bOCIW, 813 Santa Barbara St. Pasadena, CA 91101, USA

^cArcetri Observatory, Universita degli studi di Firenze, I-501125 Italy

Keywords: Visible Adaptive Optics; Adaptive Secondary Mirror; High-Contrast

ABSTRACT

The heart of the 6.5 Magellan AO system (MagAO) is a 585 actuator adaptive secondary mirror (ASM) with <1 msec response times (0.7 ms typically). This adaptive secondary will allow low emissivity and high-contrast AO science. We fabricated a high order (561 mode) pyramid wavefront sensor (similar to that now successfully used at the Large Binocular Telescope). The relatively high actuator count (and small projected ~23 cm pitch) allows moderate Strehls to be obtained by MagAO in the “visible” (0.63-1.05 μ m). To take advantage of this we have fabricated an AO CCD science camera called “VisAO”. Complete “end-to-end” closed-loop lab tests of MagAO achieve a solid, broad-band, 37% Strehl (122 nm rms) at 0.76 μ m (i') with the VisAO camera in 0.8” simulated seeing (13 cm r_0 at V) with fast 33 mph winds and a 40 m L_0 locked on R=8 mag artificial star. These relatively high visible wavelength Strehls are enabled by our powerful combination of a next generation ASM and a Pyramid WFS with 400 controlled modes and 1000 Hz sample speeds (similar to that used successfully on-sky at the LBT). Currently only the VisAO science camera is used for lab testing of MagAO, but this high level of measured performance (122 nm rms) promises even higher Strehls with our IR science cameras. On bright (R=8 mag) stars we should achieve very high Strehls (>70% at H) in the IR with the existing MagAO Clio2 (λ =1-5.3 μ m) science camera/coronagraph or even higher (~98% Strehl) the Mid-IR (8-26 microns) with the existing BLINC/MIRAC4 science camera in the future. To eliminate non-common path vibrations, dispersions, and optical errors the VisAO science camera is fed by a common path advanced triplet ADC and is piggy-backed on the Pyramid WFS optical board itself. Also a high-speed shutter can be used to block periods of poor correction. The entire system passed CDR in June 2009, and we finished the closed-loop system level testing phase in December 2011. Final system acceptance (“pre-ship” review) was passed in February 2012. In May 2012 the entire AO system was successfully shipped to Chile and fully tested/aligned. It is now in storage in the Magellan telescope clean room in anticipation of “First Light” scheduled for December 2012. An overview of the design, attributes, performance, and schedule for the Magellan AO system and its two science cameras are briefly presented here.

¹ lclose@as.arizona.edu; phone +1 520 626 5992

1.0 INTRODUCTION TO MagAO: DESIGN AND PERFORMANCE

Thanks to our past NSF MRI award **Development of an Infrared Optimized Adaptive Secondary for the Magellan Telescope** we were able to finish construction of an adaptive secondary mirror (ASM) for Magellan telescope. An additional TSIP award (**TSIP: Development of a Magellan Adaptive Secondary**) allowed us to develop a 1 kHz pyramid wavefront sensor (PWFS) for the Magellan AO system (MagAO), and also covered most of the cost of the ASM integration and testing phases for the AO system. This support allowed the MagAO system to be “end-to-end” tested over a 120 day period this year. The MagAO system itself is complete with less than 122 nm rms wavefront error in 0.8” lab seeing (see Figs 2 and 4). Lab test results will be given here. The project recently received additional support from the NSF ATI program for visible light AO science. The VisAO science case and camera will be described here as well.

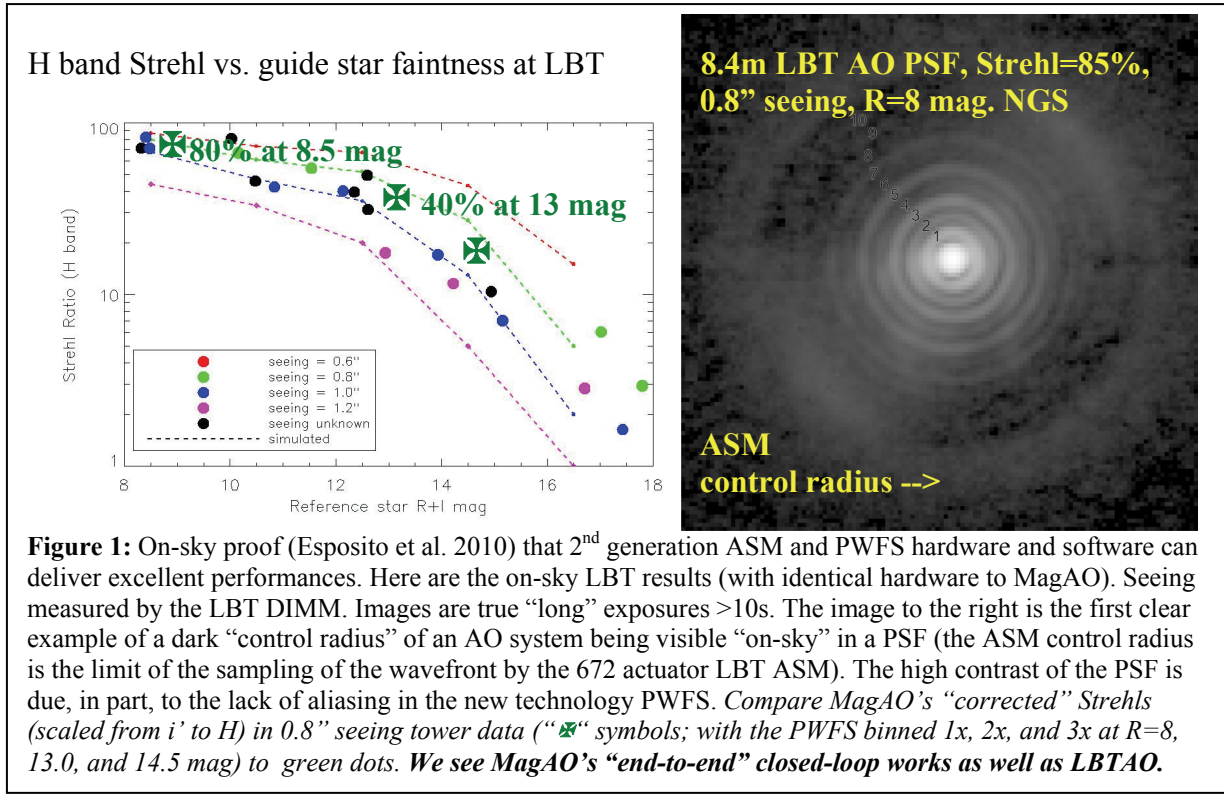


Figure 1: On-sky proof (Esposito et al. 2010) that 2nd generation ASM and PWFS hardware and software can deliver excellent performances. Here are the on-sky LBT results (with identical hardware to MagAO). Seeing measured by the LBT DIMM. Images are true “long” exposures >10s. The image to the right is the first clear example of a dark “control radius” of an AO system being visible “on-sky” in a PSF (the ASM control radius is the limit of the sampling of the wavefront by the 672 actuator LBT ASM). The high contrast of the PSF is due, in part, to the lack of aliasing in the new technology PWFS. Compare MagAO’s “corrected” Strehls (scaled from i' to H) in 0.8” seeing tower data (“x” symbols; with the PWFS binned 1x, 2x, and 3x at $R=8$, 13.0, and 14.5 mag) to green dots. We see MagAO’s “end-to-end” closed-loop works as well as LBTAO.

1.1 Past Developments of Adaptive Secondary Mirrors for Adaptive Optics

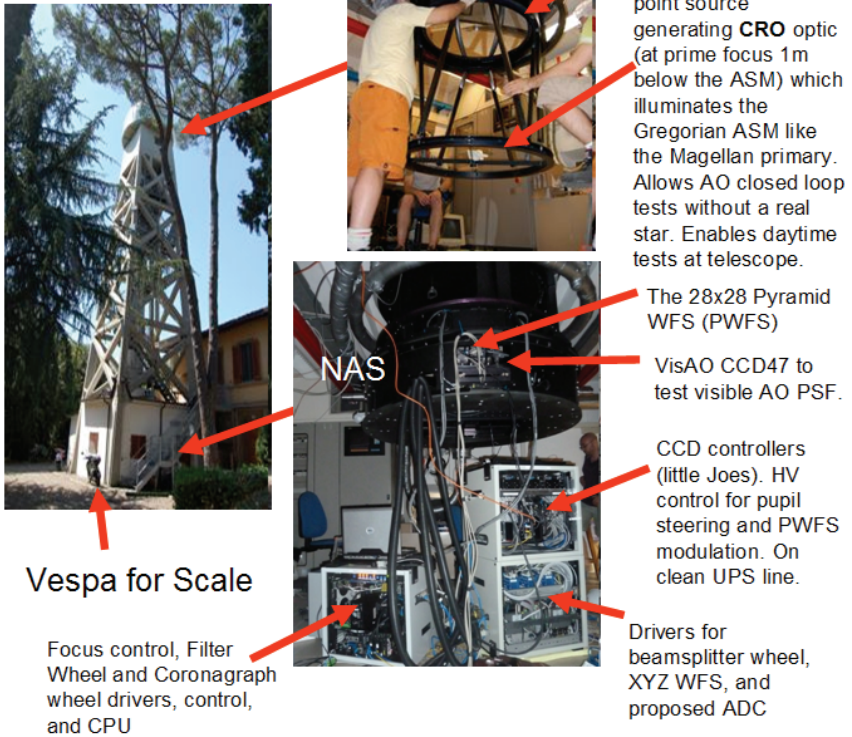
Adaptive secondary mirrors (ASMs) have several advantages over conventional deformable mirrors: 1) they add no extra warm optical surfaces to the telescope (so throughput and emissivity are optimal); 2) the large size of the optic allows for a relatively large number of actuators and a large stroke; 3) their large size enables a wide (>5') field of view (FOV); 4) the non-contact voice-coil actuator eliminates DM print-through; and hence 5) performance loss is minor even if up to ~10% of the actuators are disabled (proof: data in Fig. 1 was obtained with 20 of 672 actuators disabled). They also give better “on-sky” correction than any other AO DM (see Fig. 1). Hence, adaptive secondaries are a transformational AO technology that can lead to powerful new science and telescopic advancement (Lloyd-Hart 2000). MagAO is the result of 20 years of development by Steward Observatory and our research partner Arcetri Obs. of Italy and industrial partners Micogate and ADS of Italy.

In 2002 this Arizona/Italy partnership (Wildi et al. 2002) equipped the 6.5m MMT with the world's first ASM. This ASM is a 65 cm aspheric convex hyperboloid ULE shell 2.0 mm thick. The thin shell

has 336 magnets bonded to its backside where 336 voice-coil actuators with capacitive sensors can set the shell position. The MMTAO has carried out regular NIR science observations since 2003 reliably with little down time (see for example: Close et al. 2003a; Kenworthy et al. 2004, 2007, 2009, Heinze et al. 2010; Hinz et al. 2010). However, the MMT system was really a prototype ASM.

From the many lessons learned from the MMT's ASM, a new "2nd generation" of ASMs were fabricated for the LBT and MagAO. LBT's AO system has had a spectacular on-sky first light in June 2010 (Esposito et al. 2010) obtaining the best AO performance of a large

Fig. 2: The 14 m ASM Test Tower- Arcetri Italy and ASM & NAS



telescope to date (see Fig 1). ESO has also developed (a larger >1.0m, thicker 2.0 mm) ASM shell for their future AO facility for science use in ~2015 (AOF; see these proceedings for more info on the AOF). Also such ASMs are baselined for the 24m Giant Magellan Telescope (GMT) secondaries (~2020) and the M4 of the ~39m E-ELT (~2022), and perhaps as a future upgrade to the secondary of the 30m TMT. *Adaptive secondaries will likely play a role in all future large telescope projects.*

1.2 The 2nd Generation 585 element ASM for MagAO

Our "thin shell/voice coil/capacitive sensor" architecture is the only proven ASM approach. MagAO's "LBT-style" 2nd generation 585 actuator 85cm dia. ASM offers many improvements over the 1st generation "MMT" ASM. In particular, MagAO's successful Electro Mechanical acceptance tests in June 2010 proved that the MagAO 585 ASM has larger stroke ($\pm 15 \mu\text{m}$), a thinner shell (at 1.6 mm vs. 2.0 mm), half the "go to" time (<1ms; with electronic damping), 2-5 nm rms of positional accuracy (by use of a 70 kHz capacitive closed-loop), and just 30 nm rms of residual optical static polishing errors (compared to ~100 nm rms on the current MMT shell). These improvements are taken advantage of by LBTAO as well, but MagAO's mirror overall is slightly better behaved compared to LBT (MagAO's lack of 87 slower "outer ring" LBT actuators increases its speed w.r.t LBT). Moreover, MagAO's ASM is much more flexible than any other ASM, while also not having the inner "stressed" hole illuminated (due to the 0.29 central obscuration of Magellan). So it is not really surprising that MagAO should be the highest performance

ASM yet built – see Fig. 4 for proof of how effective MagAO is at high-order correction.

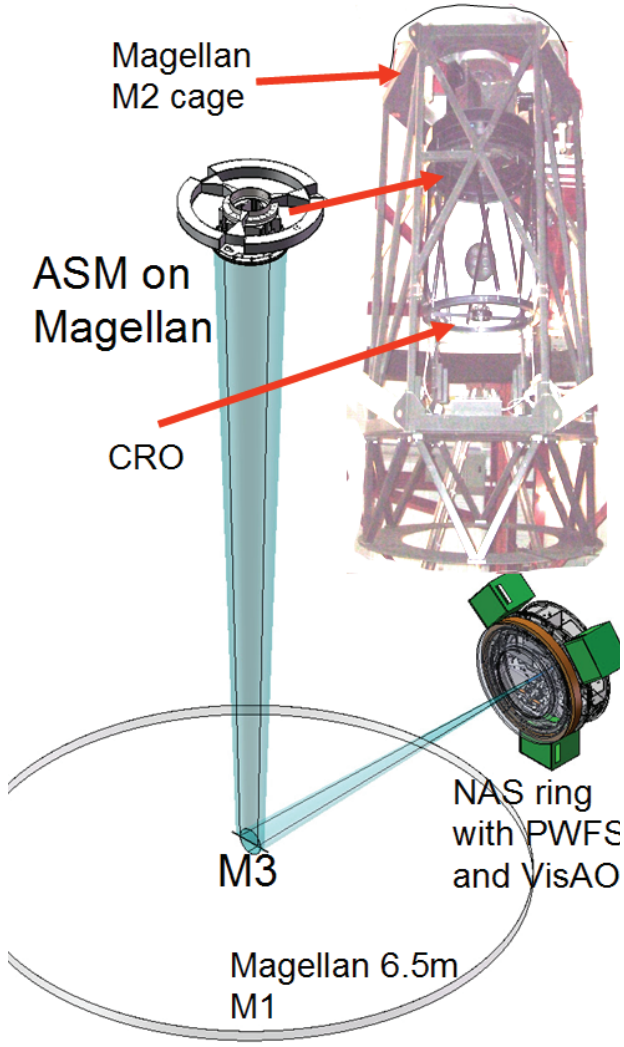
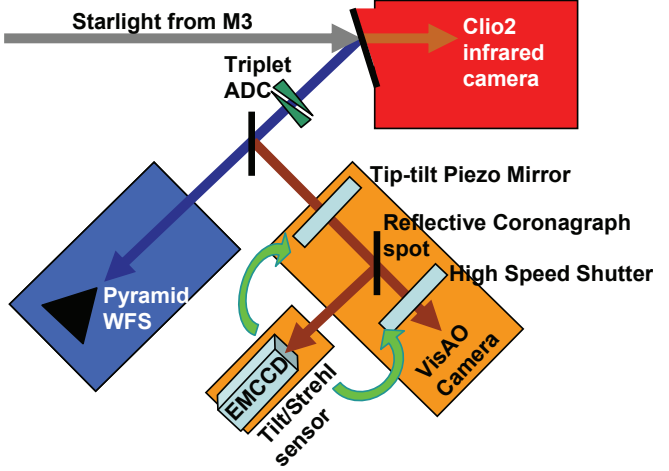


Figure 3a (left): Photo of MagAO ASM interfaces mounted for Magellan “fitcheck” run in Chile. The ASM produces a f/16 AO corrected beam which is reflected off M3 to the Clay East Nasmyth port. Mounted on the port derotator is a specially designed “NAS” (see lower right Fig. 2) housing an active optics f/16 guider, PWFS board and VisAO camera.

Figure 3b (bottom): A schematic of the MagAO system: 1) telescope light hits the dichroic window of the Clío2 IR camera, which reflects visible ($\lambda < 1.0 \mu\text{m}$) and transmits IR ($\lambda > 1.0 \mu\text{m}$) light; 2) visible light passes a triplet ADC; a dichroic beamsplitter transmits to a 28x28 PWFS; 3) reflected light feeds the AO CCD (VisAO); but 99.9% of the PSF core light can be sent to a future vibration controller.



Magellan is a Gregorian telescope and requires a large ($d=85.1 \text{ cm}$) concave ellipsoidal ASM. The concave shape of a Gregorian secondary enables easy testing “off the sky” with an artificial “star” (see the test tower in Fig. 2). In addition, 585 mode servo loop CPU latency is limited to $<120 \mu\text{s}$ through the use of 336 dedicated DSPs (producing ~ 250 Giga Flops, in the ASM electronics) for very fast real-time performance.

1.2 Current Status of the MagAO System

The entire MagAO system passed a rigorous PDR (Dec 5, 2009) and an external CDR (May 28, 2009). The PI and MagAO team relocated to Italy for half of 2011 and completed the Integration and Testing phase of the project. All telescope interfaces (ASM mount, NAS mount, M2 cooling lines, etc) were successfully tested at Magellan’s Clay telescope during a 4 night “fit check” run in Dec. 2010. Today all key MagAO systems have been fabricated, integrated and tested. All MagAO components (including

MagAO's VisAO PSF is excellent: 55% Strehl lab (>37% "sky") at i' (0.76 μm)

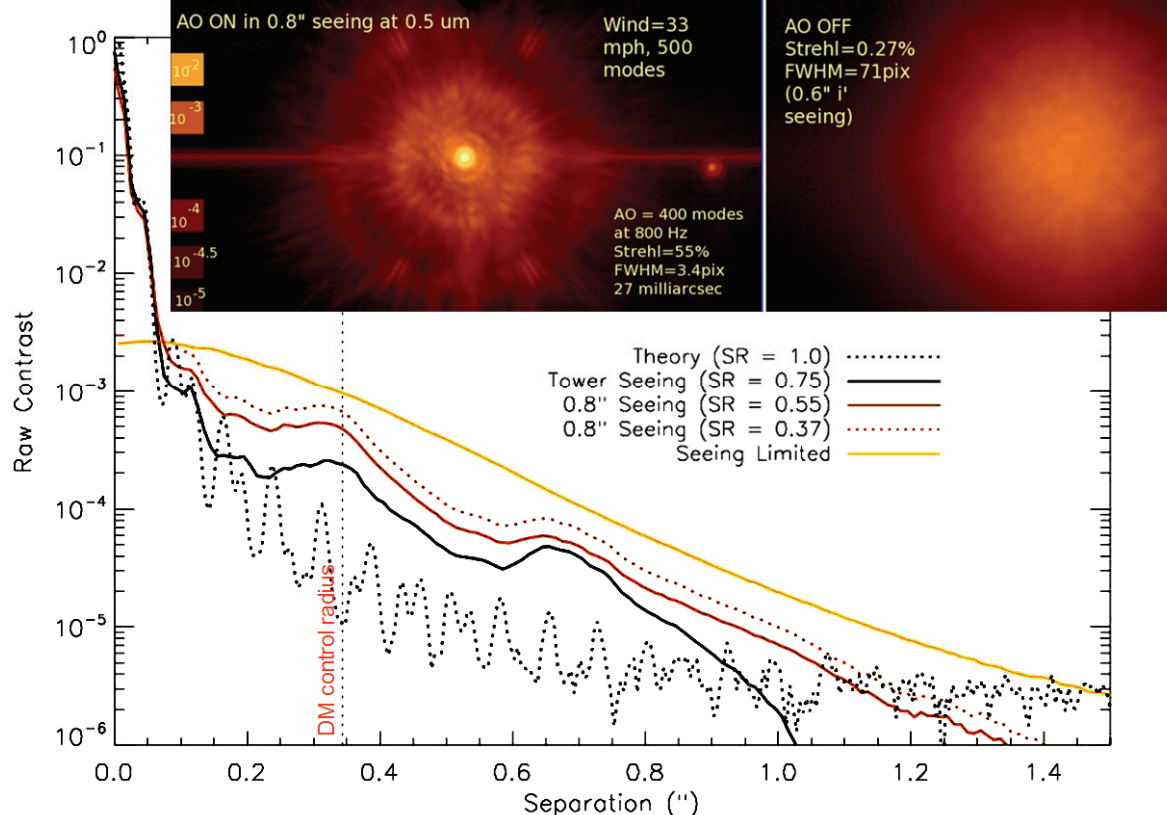


Figure 4: Real closed loop “end-to-end” Tower tests of MagAO at i' (0.76 μm) with prototype VisAO camera. Inset Left to Right 1) a deep 120s exposure with AO “on” (400 controlled modes, 800 Hz) with 500 modes of injected 0.8'' V band seeing and 33 mph winds with Lo=40m ($R=8.1$ mag “star”). Gives a raw Strehl=55%; which “corrects” to >37% (122 nm) when considering that mirror fitting error is missing modes >500); and 2) AO “off” (ASM static but good) with same seeing yields just SR=0.27%. **These results show that in >75%-ile of seeing we will achieve > 37% Strehl (on axis, low airmass, no vibrations) at i' (and longer λ) with bright $R<10$ mag NGSS at Magellan.**

observatory software) have been “end-to-end” close-loop tested in the 14m Test Tower (see Fig. 2) in Italy by the MagAO team and our Arcetri collaborators (see Fig. 4 for a typical test tower VisAO PSF image). The system has now been successfully shipped to Chile (LCO). After shipping all systems were retested and aligned successfully (May 2012). The system will have first light on the 6.5m Clay telescope in December 2012.

The schematic drawing above (Fig. 3b) outlines how our VisAO and Clio2 cameras are co-mounted and can be used simultaneously (if desired). No instrument changes are ever needed to switch between IR and visible science. In the campaign/queue mode envisioned for MagAO one will not use VisAO if seeing is poor, nor will any telescope time be lost since 1-5.3 μm Clio2 science can be done in >90% of the seeing conditions at Las Campanas --an excellent (median $V=0.64''$) seeing site (Thomas-Osip 2008).

2.0 OUR APPROCH TO VISIBLE LIGHT AO

2.1 MagAO's VisAO Camera vs. HST, Interferometers, or NIR AO on 8-10m Telescopes

MagAO's 2nd generation secondary creates a tremendous opportunity to regularly obtain moderate Strehl and 20 mas resolution images in the visible (see Fig. 4). *This is 2.7x higher resolution than the Hubble Space Telescope can achieve at the same wavelengths, and is also ~2-3x better than the sharpest images one can make from the ground with conventional NIR AO on the largest 8-10m apertures.* While interferometers can provide higher spatial resolutions, their limited "uv" coverage, limiting magnitudes, and very small FOV (<0.1") make them generally much less attractive than direct imaging for the science cases outlined in section 2.3. Also, speckle interferometry can achieve the diffraction-limit, but is only effective on the brightest binary stars in the optical, with limited contrast and, hence, dynamic range.

**TABLE 1: Science/Technical capabilities of the VisAO Camera
(component status: “finished” or “in development”)**

High order DM (finished)	585 1kHz actuator ASM > $\pm 15\mu\text{m}$ stroke
AO PWFS with high order corr. E2V 80² CCD39 (Finished)	1kHz Pyramid 28x28 WFS, scalable from: 49-561 modes (allows faint R=16 mag natural guide stars NGS). Large 200" dia. FOV patrol field for NGS PWFS
VisAO CCD (finished)	1k ² E2V 95% QE “midband” coated CCD47-20
VisAO CCD camera optics (finished)	8.0 mas/pix, 8x8" FOV, <30 nm rms static wavefront error
Vibration control (in development)	>500 Hz tip-tilt image EMCCD stabilization system
Smart Shutter (finished)	>10 Hz shutter system to block bad seeing.
Super ADC (in development)	Allows Broad Band high airmass observations with no image wobble (prototype finished)
High quality Filters & Polarizers (finished)	r', i', z', "y", SDI_Ha, SDI_[OI], SDI_[SII], Wollaston polarizer
Anti-sat. Coronagraph Masks (r=0.1" ND3 mask is finished)	r=0.1", 0.5", 1.0", 2.5" spots, ND3, ND4, ND5
High Speed, VisAO Modes: (finished)	Bright star: Shutter limited Int. <3 ms. (3e RON) Lucky: 512x512 20Hz (5e RON) up to 500 Hz

A simple reason that many “VisAO” science cases cannot be done with HST is that the brightest science targets (V<8th mag) become difficult to observe without debilitating core saturation/charge bleeding -- even for minimum exposures. Moreover, the permanent loss of the ACS HRC channel leaves just the visible coronagraphic “wedge” in STIS on HST. With a size of >0.2", which often covers up the most important science area for circumstellar science (the core), this bar inhibits HST study of our “VisAO” science cases. **Our goal is to provide a 2-3 fold improvement in the angular resolution of direct imaging in astronomy while simultaneously gaining access to the important narrowband visible (0.6-1.05 μm) spectroscopic features that have been inaccessible at 0.02" resolutions to date.** VisAO is very competitive with future instruments: with >3x finer resolution and sampling (0.008"/pix) than the future Hale 5m PALM-3000 SWIFT IFU and >3x higher Strehls and resolutions than the future (~2015?) European AOF MUSE IFU. VLT’s future (~2013) ZIMPOL could be competitive with VisAO --but it is really a dedicated 3x3" polarimeter. In the future Keck’s proposed (but not yet fully

funded) NGAO could have higher resolution (and LGSSs), but is located in the North (like PALM-3000) and limited to $\lambda > \sim 0.8\mu\text{m}$.

2.2 Our Simulated MagAO/VisAO Error Budget Compared to Test Tower Results

MagAO's 585 controllable modes map to a 23 cm "pitch" on the 6.5m primary. This is a smaller

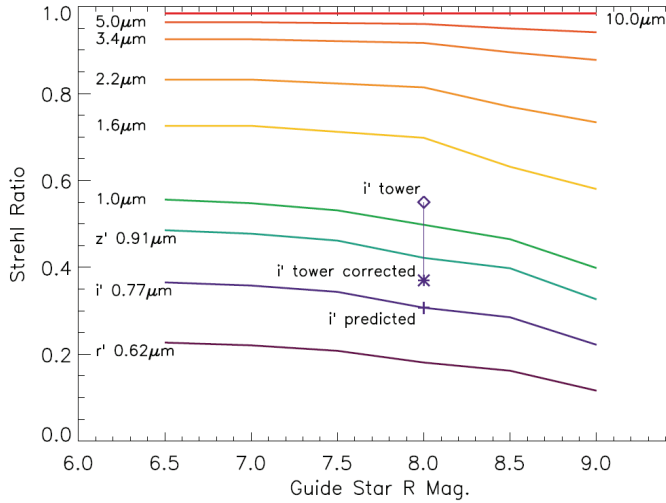


Figure 5: Numerical simulations of the MagAO Strehl vs. guide star R mag. For $R < 9$ mag we will achieve $SR \geq 30\%$ in the i'' band. These curves assume the same parameters as shown in Table 2. For fainter 13 and 15th mag NGSSs see the green crosses in Fig. 1 for the faint star lab values..

Table 2: Error Budget (nm rms) for Mag AO system for a R=8 mag NGS. $\lambda=0.76\mu\text{m}$		
Term	CAOS value	Notes (red terms have been independently measured in lab.)
Fitting	91	$r_0=14$ cm @V "poor" (75%-ile) 0.8" seeing
Servo	55.4	800 Hz framerate
Recon.	47.0	11e RON (<i>9e in lab</i>)
Static	30	<i>Verified by 4D int.</i>
Noncom	29.0	<i>estimated by 4D in lab.</i>
tilt	52.6	5 mas –Assuming Vibration Control active if windy
Total (rms) wavefront	135	96 nm obs. in Tower. <i>Corrected to 122 nm for all modes > 500 as well.</i>
Strehl 0.76μm	30%	37% expected on sky correcting from lab.

Fit: 561 illuminated act. controlling 400 modes

(tighter) pitch than all current AO systems (even 20% smaller than the LBT). To predict the exact degree of correction we used "end-to-end" simulation of MagAO/VisAO with the Code for Adaptive Optics Simulation (CAOS; Carbillot et al. 2005). Our CAOS simulations (assuming no extra telescope vibration) predict slightly larger wavefront errors (135 vs. 122 nm rms) than our "corrected" test tower results (Col. 2 vs. Col 3. Table 2), hence our tower results are quite consistent with our analytical model of MagAO.

2.2.2 Moderate Strehls robustly obtained in the Visible with LBTAO on-sky

While simulations, and lab tests give significant comfort, the true test is whether the AO system can actually achieve $>30\%$ Strehls reliably in median atmospheric conditions (0.7") on the sky. Since spring 2009, a near clone of our AO system and WFS (the LBTAO#1 system) has been tested on-sky. During first light the LBT saved a few visible images of stars with its undersampled "technical viewer" CCD. This camera is not designed for VisAO science, however, the LBTAO system was able to consistently record long exposure (>6s) 20% Strehl images at $0.85\mu\text{m}$. **The consistency of the MagAO closed loop lab tests with our simulations and the promising on-sky "first light" results of LBT's technical viewer (without use of ADCs, vibration elimination, or even Nyquist platescales) give us great confidence that MagAO's VisAO camera will achieve the performances predicted here.**

2.3 A Few Selected Science Cases for Visible AO Imaging (VisAO) Observations

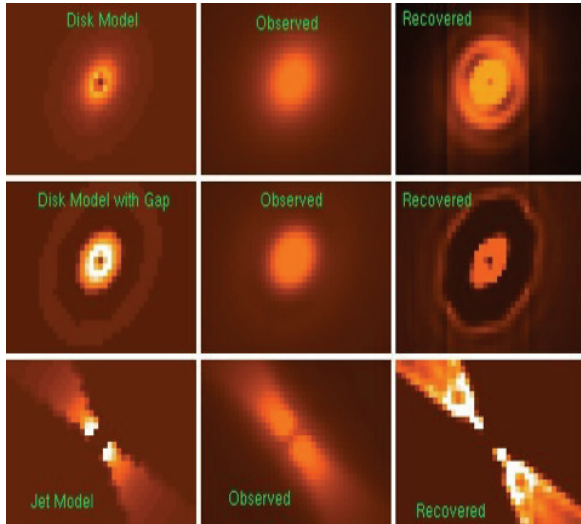


Fig 6: (left) Disk, gap, and jet [OI] models for HD101412. (middle) Models convolved with 10% Strehl PSF. (right) deconvolved 8.5 mas/pix SDI “on” [OI] images. The S/N of the images is for a 20 minute simulated SDI int. on HD101412’s known r~10 AU [OI] disk. Even with low SR PSFs VisAO can recover ~20mas complex dust & jet structures thanks to a well known continuum PSF from SDI.

structure and its connection to the process of planet formation (a top science recommendation of ASTRO 2010). The SDI “trick” here is that the hot star is pure continuum at 6300A, so simple SDI continuum subtraction will remove the star (to the photon noise limit) yet reveal the disk (and/or jet) in emission. We investigated the suitability of VisAO SDI to attack the question of disk morphology with a preliminary study of the type of disk structure that will be resolvable with VisAO in SDI mode. We simulated SDI images (with noise) of a protoplanetary disk around a typical Herbig Ae/Be star at the 120 pc distance of the ρ-Oph star forming region using smoothed versions of the radial profiles (r~10 VisAO pix) inferred by van der Plas et al. We simulated: a disk, a disk with a gap from 5-10AU and a jet. Fig. 6 (middle) shows simulated [OI] 6300A images of these three cases (assuming a conservative 10% Strehl 0.63μm VisAO PSF made by CAOS in 75%-ile seeing). The stellar continuum (and PSF) is easily isolated with the SDI “off” filter. This PSF is then used for deconvolution, and even with a forced 20% PSF mismatch, the recovered images look great in the right of Fig. 6. *The SDI mode will be a uniquely powerful tool for understanding jet creation and collimation and the structure of circumstellar disks and gaps, morphology too complex for interferometry alone.* A well designed SDI survey of the 45 closest (<150 pc) brightest circumstellar disks (in [OI] and H α) and jets (in [SII]) with bright cores (R<10 mag) is a key project goal.

In-fact, given an R<10 NGS we can image any emission/absorption line system at 20mas. Some other SDI surveys will include: Evolved II-IV class stars; AGB stars, Eta Car and other LBVs; a survey of 210 close O,B,A stars for faint H α active late-type companions, and some of the 1020 R<5 mag stars <100pc dec<20). Such large narrowband, high-contrast, surveys cannot be done with today’s AO systems.

2.3.1 Herbig Ae/Be Disks Resolved by VisAO SDI

Our VisAO CCD will make unprecedented high-contrast disk images with Spectral Differential Imaging (SDI a simultaneous imaging “in” and “out” of, for example, H α). See Close et al. (2005) for background on SDI and sec 2.3.6 for the optomechanical details. We will open up an exciting frontier in the high-contrast study of Herbig Ae/Be circumstellar disk & jet structure. Our VisAO system can resolve >50% of disks around known nearby young massive stars (for example 27/47 of the Hillenbrand et al. (1992) sample are good R≤10 mag NGS). According to recently published models, photoionized disk atmospheres are expected to radiate detectable amounts of forbidden line emission (Ercolano et al. 2008). The [OI] 6300 Angstrom line has been spectrally resolved in such disks with UVES on the VLT (van der Plas et al. 2008), however spatial information can currently only be guessed at. *The ability to spatially resolve complex disk morphologies like gaps, jets and flaring would aid greatly in our understanding of disk & jet*

2.3.2 High-Contrast H α Emission Line Imaging of Accreting Extrasolar Planets

Another key survey project we would like to do with VisAO is high-contrast H α SDI imaging of the emission from the accretion shock caused by gas accreting onto gas giants during formation. We'll target >100 known southern, young (<10 Myr), nearby (<150 pc), gas-rich systems that have $I \leq 10$ mag. During the time of gas accretion the protoplanets will have $\sim 10^{-(3-4)} L_{\text{sun}}$ and much of this will be radiated at H α for $\sim 10^6$ yrs (Fortney et al. 2008). In this manner, we can finally directly image giant planets where/when they form (likely past the “snow-line” >30 -50 mas) as H α point-sources orbiting the young target star.

2.3.4 High-Contrast Imaging of Extrasolar Planets in the Habitable Zone of Nearby Planets

An other Key Project for the VisAO camera will be to take deep ADI datasets on nearby stars to directly detect reflected light from giant planets. We have formed a strong group of scientific collaborators from across the Magellan Partnership to make sure that such a survey is well designed and will obtain the telescope resources required to finish. We can detect Eps Eri b in an ideal (photon noise limited) 10 hr ADI exposure, using orbit of Benedict et al. 2006, and albedos model of Cahoy et al. 2010 – orbital phase (planet illumination) and true separation are all correctly treated.

2.3.5 Asteroid and Solar System Surfaces, and Titan’s Atmosphere

There are many science cases where simply mapping objects at these very high resolutions is exciting. For example, even moderate Strehls are fine for mapping the edges of astroidal surfaces with the VisAO imager. The VisAO camera can also map Titan (diameter $\sim 0.7''$) with a $0.95\mu\text{m}$ CH₄ filter.

2.4 New components: Development of a “Telescope Ready” VisAO Camera

In addition to 1kHz frame rates and a 585 actuator ASM, we also need: 1) better ADCs (to work at low elevations); 2) “smart” fast shutters (to block periods of bad Strehl); 3) small ND reflecting coronagraphic masks (to keep the core of the target from saturating our CCD47 science camera; and 4) super-compact, liquid cooled, fast EMCCD tilt sensors for *active* vibration elimination --by guiding off the light reflected by the coronagraph. These results will help open up the field of visible AO for future AO systems on large telescopes. See Fig. 8 for our full VisAO opto-mechanical design.

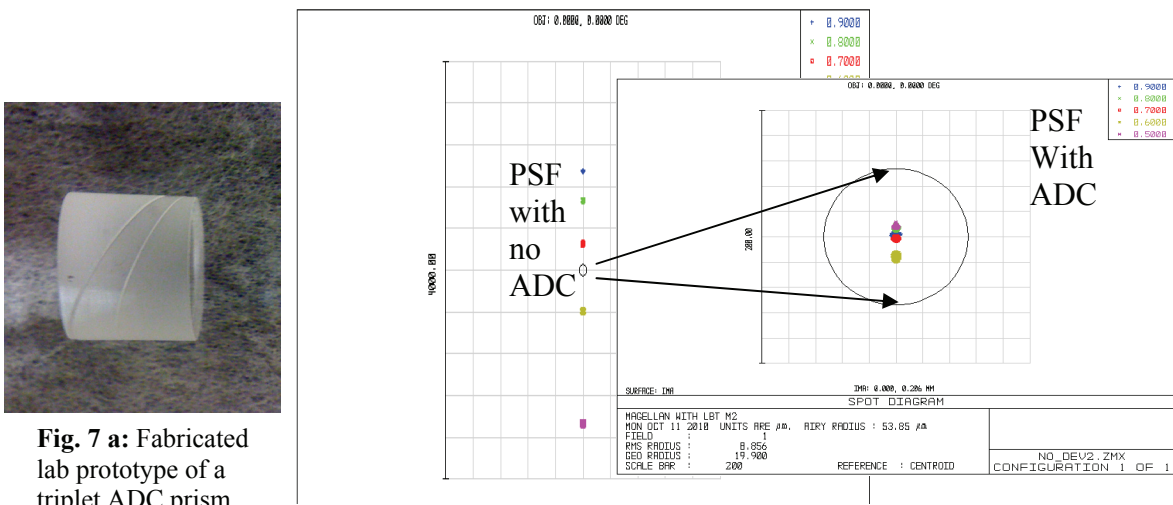


Fig. 7 a: Fabricated lab prototype of a triplet ADC prism. It had great dispersion, but also had some image wobble as the ADC rotates (Kopon et al. 2010).

Fig. 7 b: The new “super” ADC design (with 5 precision $\pm 1'$ wedges) performance at 2 airmasses (with no image wobble). Without ADC the $0.5\text{-}0.9\mu\text{m}$ PSF on the PWFS is $>3000\mu\text{m}$! With the new ADC the PSF has $<45\mu\text{m}$ of dispersion ($<28\text{ mas}$).

2.4.1 New VisAO ADC Design: The “super” ADC

Most ADCs designed and built to date consist of two identical counter-rotating prism doublets. The indices of the two glasses are matched as closely as possible in order to avoid steering the beam away from its incident direction as the components rotate. The wedge angles and glasses of the prisms are chosen to correct primary chromatic aberration at the most extreme zenith angle. By then rotating the two doublets relative to each other, an arbitrary amount of first-order chromatic aberration (lateral color) can be added to the beam to exactly cancel the dispersion effects of the atmosphere at a given zenith angle. The standard 2-Doublet design corrects the atmospheric dispersion so that the longest and shortest wavelengths overlap each other, thereby correcting the primary chromatism. Secondary chromatism is not corrected and is the dominant source of error at higher zenith angles. To correct higher orders of chromatism, more glasses and thereby more degrees of freedom are needed.

In our 2-triplet design (see Fig. 7), a third glass with anomalous dispersion characteristics (Schott’s N-KZFS4) is added to the crown/flint pair. Like the doublet, the index of the anomalous dispersion glass was matched as closely as possible to that of the crown and flint. The three wedge angles of the prisms in the triplet were optimized to correct both primary and secondary chromatism. A lab prototype (Fig 7a) matched the Zemax dispersive atmospheric color exactly (Kopon et al. 2010). Yet we have added an addition 2 wedge cuts into the outer faces to minimize any deviation of the image as the ADC rotates. See Kopon et al. 2012 (these proceedings) for more details.

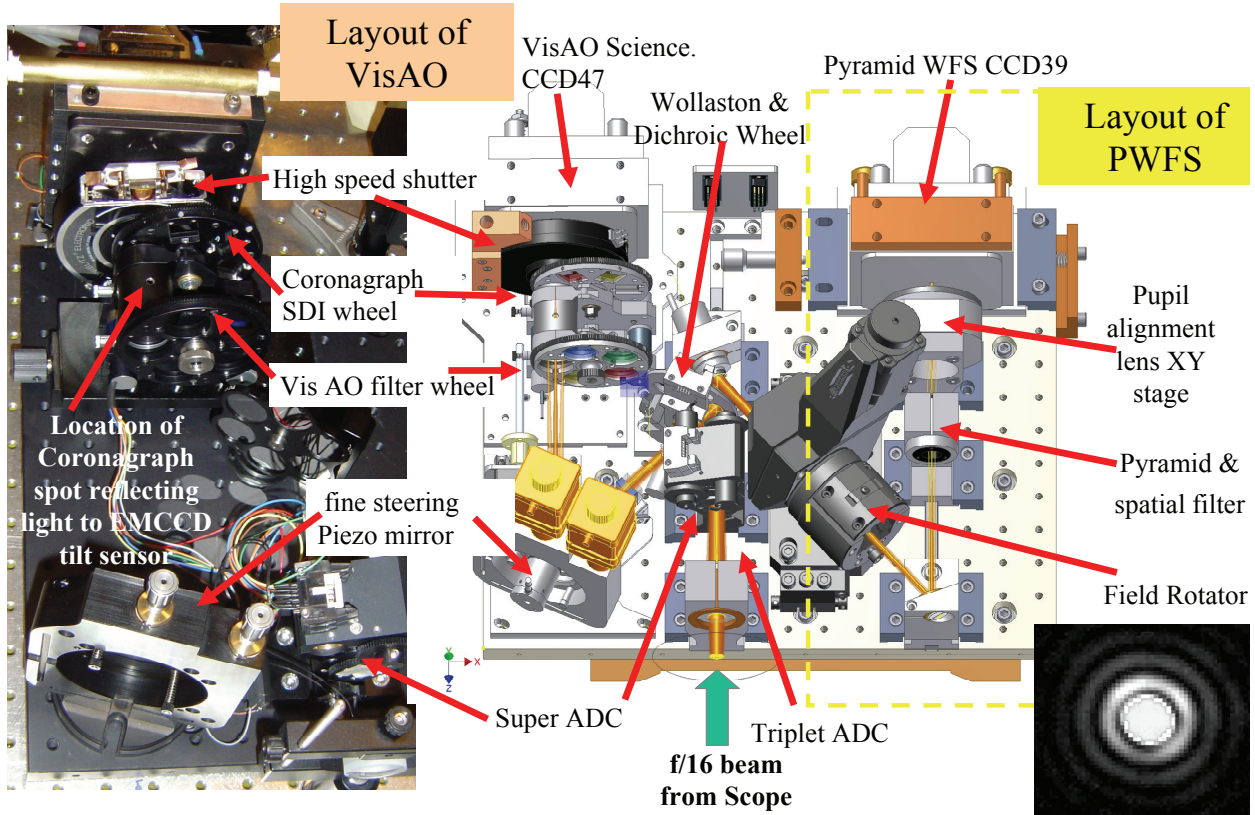


Figure 8: Our VisAO prototype camera (*lab photo*). Detector is a $1k^2$ E2V CCD47 with 8.0 mas/pix. The VisAO is rigidly “piggybacked” on the same rigid optical table as the PWFS (detector: 80x80 E2V CCD39, 9e-RON 1KHz framerate), hence non-common path aberrations and vibrations are minimized. The light is split at the dichroic beamsplitter wheel. Only the missing VisAO parts (see Table 1, or Budget Justification, for parts list) require support from this ATI. The PWFS side (inside yellow dashed box) is completely finished and tested in the Tower (see Fig 2) –shown here as a CAD image for clarity that a photo does not have. *Inset* VisAO PSF for $\lambda \geq 0.53\mu\text{m}$ (Strehl>96%) with no turbulence.

Using the on-axis rms spot size over the broad band $0.5\text{-}1.0\ \mu\text{m}$ as the figure of merit, our new “super” 2-triplet performs $>58\%$ better at high airmass ($>1.5\ \text{AM}$) than a conventional 2-doublet design (compare both figs in 7b). **This will allow diffraction-limited broadband imaging at the VisAO focal plane and much better pyramid WFS performance (with a very broad $0.5\text{-}1.0\mu\text{m}$ PWFS bandpass) by producing a more focused λ/D spot at the pyramid tip (see right side of Fig 7b).** This will be particularly important in the case of good seeing and low PWFS modulation amplitude ($\pm 2\lambda/D$) of the star around the pyramid tip --critical for successful VisAO.

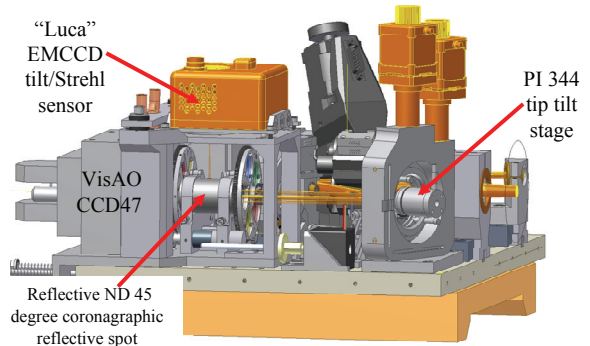


Fig 9: Side view of VisAO with a future Luca Electron Multiplication (EMCCD) tilt CCD shown. The Luca forms a PSF image from the light reflected off the coronagraphic ND spot.

2.4.2 Reflective ND Coronagraphic Spots/masks

With Reynard Corp. we are expanding on the work of Park & Close et al. (2006) and developing a new type of commercial coronagraph that is a metallic reflective neutral density (ND3-ND5) “spot”. When deposited on a 45 degree flat plate, the ND3 spot will reflect 99.9% of the inner $r=0.1''$ to prevent saturation of the target core on the CCD47 (this coronagraph is actually critical for $R \leq 10$ mag targets to allow ≥ 5 s integrations without saturating the core– hence it is always needed for VisAO). The light reflects into the future Luca EMCCD tilt sensor. The 45° flat is in the “tube” below the Luca in Fig 9.

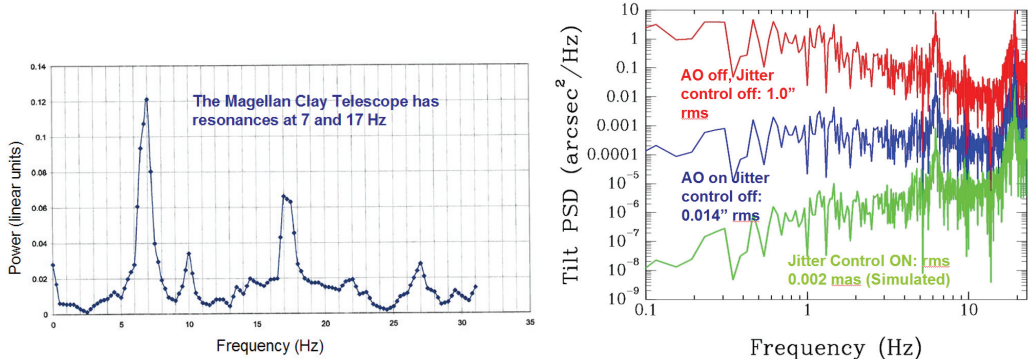


Fig. 10: (left) the telescope power spectra, (right) real tilt PSD with 0.8" seeing and 7 and 17 Hz resonances injected into the tower turbulence. Note that only a 532Hz vibration (jitter) control loop can keep VisAO diffraction-limited in windy conditions. Hence our need for a future vibration control system shown in Fig. 9.

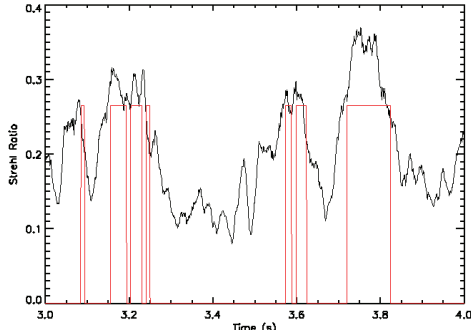


Figure 11: Numerical timeseries simulations. This plot illustrates the short term temporal variability of SR at 0.7 μ m. Overlay in red is the actual response of our shutter guided by a simulated Luca EMCCD tilt/Strehl camera. Note how only SR>25% is seen by VisAO CCD.

that these “Luca” images will also allow the real-time VisAO Strehl to be measured and the fast shutter can be asynchronously controlled at ≤ 100 Hz to block bad periods of seeing.

2.4.5 A New Smart Shutter to Enable Higher Strehls in Long Exposures

The benefits of selecting images based on SR have been demonstrated through the well-known “Lucky” Imaging technique (Law et al, 2009). This technique requires reading the detector at high speed to catch periods of high SR without being contaminated by the periods of low SR. For bright objects, we have the ability to read the CCD47 at fast rates (20 Hz, 512² window, <5e RON). This capability facilitates a “Lucky imaging”-style data reduction technique when read noise is not limiting.

2.4.3 Vibration Control with a Custom EMCCD Andor “Luca” tip-tilt/Strehl Camera

We are planning to modify Andor’s “Luca R” to produce an ultra-compact “gain” EMCCD (Andor’s standard cooling fan will be replaced with a custom liquid cooling). This camera (6.5 mas/pix) will be binned and windowed to a selectable 88x64 ROI (0.57x0.42") with >500 Hz framerates (1 ms integrations) to drive the tilt loop (which is safely below the resonance of the loaded PI 334 piezo tip-tilt stage). In Figure 10 we show how known telescope resonances at 7 and 17 Hz (beyond 17 Hz the scope is quiet) can be controlled with the vibration control system (simple integrator model; Roddier 2000). The digital servo system will be tuned to not amplify the small amount of residual jitter for $f > 30$ Hz. We note

For fainter, RON-limited observations, we can use the LUCA EMCCD (see Fig 11) to monitor the Strehl in real time and trigger our fast shutter when the Strehl falls below our threshold (of, say, 30% Strehl). Currently this is done by estimating the Strehl in real time from the PWFS slopes. With our shutter (a Uniblitz VS-25; capable of 5 msec exposures), this is equivalent to operating our 1kx1k CCD47 at 200 Hz in “Lucky mode” with negligible read noise! So the CCD47 simply integrates we control the shutter (See Males et al. 2012 (these proceedings) for much more details on real shutter lab tests). In this manner, the VisAO camera will be able to obtain long exposure 20-40% Strehl images in the optical --opening the regime of deep 20 mas imaging for the first time. An important consideration in frame selection is the telescope duty cycle (which we lack the space to discuss here). Males et al. (2010) discusses efficiency vs. resolution tradeoffs using "Real Time Frame Selection" techniques and the results of lab characterization of the shutter and control algorithms. See Males et al. 2012 (these proceedings) for more details.

2.4.6 The VisAO Camera: Coronagraphic and SDI Modes

As is clear from Figure 8, the VisAO design incorporates all the key features and remotely-selectable elements necessary to optimize VisAO science. In particular, the coronagraph wheel will contain a range of our custom reflective ND masks (Park et al. 2007), allowing deep circumstellar science on bright targets that would otherwise saturate the detector. The main purpose of these masks is to prevent blooming of the CCD47 detector and feed the EMCCD tip-tilt sensor/Strehl monitor. Our coronagraph doesn't need to suppress diffraction rings since the ADI/LOCI reduction technique work very well. In general, the number of useful astrophysical investigations possible with Strehls in the ~20-40% range are limited without accurate PSF calibration.

One needs simultaneous PSF information to compare to (or deconvolve against) the “in-line” science image. An extremely effective technique for this is Simultaneous Differential Imaging (SDI; Close et al. 2005) which utilizes a Wollaston Beamsplitter to obtain nearly identical, simultaneous, images of the *o*-polarized and *e*-polarized PSFs (typically there is <10 nm rms of non-common path SDI error between the *o* and *e* images; Lensen et al. 2004; Close et al 2004). The SDI configuration of the VisAO camera includes: 1) a future 4x8” field stop in the telescope’s f/16 focal plane; 2) a thin small angle calcite Wollaston beamsplitter near our pupil; and 3) a split on-H α /off H α “SDI” filter just before the focal plane (for the *e* beam/*o* beam). In this mode, we have obtained an almost perfect (photon noise limited) simultaneous calibration of the PSF “off” and “on” the H α line in the lab. Hence, a simple subtraction of the “off” image from the “on” image will map H α structures (jets, disks, accreting faint companions etc), with minimal confusion from the continuum or PSF. We will have four such SDI filter sets (with optional SDI double spot coronagraphic masks) for the H α , [OI], and [SII].

3.0 A 1-5 μ m SPECTROGRAPH AND CAMERA –CLIO2

We have (in the test tower lab) made a convincing case that our PWFS + 2nd gen. ASMs like LBT has residual wavefront errors of <130nm (>94-97% SR at L-M). Hence, very high Strehl can be achieved at H band through M band with high-contrast imaging being possible with bright (R<12) stars. Prof. Phil Hinz has developed a facility high-contrast coronagraphic camera, Clio2, which has been the 1-5.3 μ m imager with MMTAO since 2006. Clio2 has full 1-5.3 μ m filter sets, unique 10^5 contrast APP coronagraphic phase plates (Kenworthy et al. 2007, 2009) and future Lyot coronagraphs. These coronagraphs should yield $>10^5$ contrasts past 0.5-1.0” with MagAO. Clio2 is already a fully functioning

camera (in June 2010, Clio was upgraded to Clio2 with a 1-5.3 μ m Hawaii 1024x512 MBE detector). With support from our new ATI award we have modified Clio2 to be a world class high-contrast AO camera and spectrograph for Magellan. Clio2 can now mount on the back of the NAS and fully rotate as a Nasmyth facility IR camera. In the future a 8-26 micron camera (MIRAC4) will be used as well.

Table 3: The MagAO 1-5.3μm IR Camera Spectrograph: Clio2	
Spatial platescale, FOV at Magellan	18 mas/pix or 30 mas/pix, FOV: 18x9" or 30x15"
Filters (see http://zero.as.arizona.edu/clio)	J, H, Ks, K, L, L', L_ICE, L_CH4, M, M'
Spectra Resolution with Prism	R~130 at L
Est. (Ks) 1 hr 5σ point source \leq12 mag NGS	23.9 mag r<10" off axis, if r>20" Ks~22.2

3.1 An Upgraded Clio2 for MagAO: Unique Exoplanet Follow-up Capabilities in the South

Clio2 is already a functioning AO science camera (PI Phil Hinz); however, it is now upgraded with a motorized platescale changing drive. Clio2 will be the only L & M band follow-up spectrograph to probe CH₄/CO ratios of extra-solar planets that will be discovered by Gemini's GPI and VLT's Sphere (neither have any capacity at the CH₄ fundamental at 3.3 μ m, L or M band). Team member, Katie Morzinski is also GPI exoplanet campaign Co-I and will lead this follow-up effort as part of her Sagan Fellowship. This is just one example of where Clio's unique L & M high Strehl capability in the southern hemisphere will be critical for one of the top science goals of ASTRO2010 "Characterization of extrasolar planets". Many other general NIR science cases will be executed by Clio2.

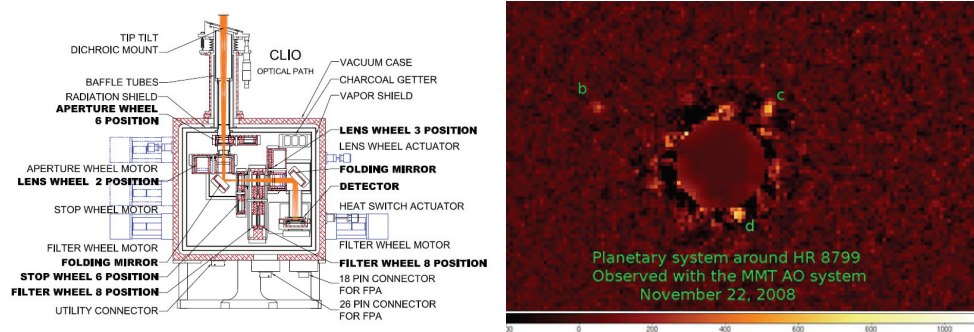


Fig 12: Cross-section of Clio2. Clio has already been used for high-contrast science, note the L band ADI image three extrasolar planets in the HR 8799bcd system taken with Clio and MMTAO (Hinz et al. 2010).

REFERENCES

- Agapito et al. 2008, SPIE, 7015, 70153G
- Brusa G. et al. 2003 proc SPIE 4839, 691.
- Burges C.J.C. "A Tutorial on Support Vector Machines for Pattern Recognition". Data Mining and Knowledge Discovery, Vol. 2, No. 2, pp 121-167, (1998).
- Benedict, G.F. et al. 2006 AJ 132, 2206
- Carbillet, M., et al. "Modeling astronomical adaptive optics - I. The software package CAOS", MNRAS, Volume 356, Issue 4, pp. 1263-1275 (2005).

- Carbillet, M., et al. "Performance of the first-light adaptive optics system of LBT by means of CAOS simulations", SPIE Proc. 4839, 131 (2003).
- Close L.M. et al. 2005b NATURE 433, 286
- Close L.M. et al. 2003a, ApJ 599, 537
- Close L.M. et al. 2003b ApJ 598, 35L
- Close, Laird M.; Gasho, Victor; Kopon, Derek; Hinz, Phil M.; Hoffmann, William F.; Uomoto, Alan; Hare, Tyson, 2008 Proc SPIE Volume 7015, pp. 70150Y-70150Y-12
- Close, Laird M.; Gasho, Victor; Kopon, Derek; Males, Jared; Follette, Katherine B.; Brutlag, Kevin; Uomoto, Alan; Hare, Tyson, Adaptive Optics Systems II. Edited by Ellerbroek, Brent L.; Hart, Michael; Hubin, Norbert; Wizinowich, Peter L. 2010 Proceedings of the SPIE, Volume 7736, pp. 773605-12
- Cahoy, Kerri L.; Marley, Mark S.; Fortney, Jonathan J. 2010, ApJ 724 189
- Ercolano, B., Drake, J. J., Raymond, J. C. & Clarke, C. C. 2008, ApJ, 688, 398E.
- Esposito S. et al. 2006 Proc. SPIE Volume 6272, pp. 62720A
- Esposito, Simone; Riccardi, Armando; Fini, Luca; Puglisi, Alfio T.; Pinna, Enrico; Xompero, Marco; Briguglio, Runa; Quirós-Pacheco, Fernando; Stefanini, Paolo; Guerra, Juan C et al. 2010 Adaptive Optics Systems II. Edited by Ellerbroek, Brent L.; Hart, Michael; Hubin, Norbert; Wizinowich, Peter L. Proceedings of the SPIE, Volume 7736, pp. 773609-12
- Ferrarese, M. & Merritt, D. 2000, ApJ, 539L, 9F.
- Follette, Katherine B.; Close, Laird M.; Kopon, Derek; Males, Jared R.; Gasho, Victor; Brutlag, Kevin M.; Uomoto, Alan, 2010 Ground-based and Airborne Instrumentation for Astronomy III. Edited by McLean, Ian S.; Ramsay, Suzanne K.; Takami, Hideki. Proceedings of the SPIE, Volume 7735, pp. 77351P-10
- Fortney, J. J.; Marley, M. S.; Saumon, D.; Lodders, K. 2008 The Astrophysical Journal, Volume 683, Issue 2, pp. 1104-1116.
- Gebhardt et al. 2000, ApJ, 529L, 13G.
- Gratadour, D., Rouan, D., Mugnier, L. M., Fusco, T., Clenet, Y., Gendron, E. & Lacombe, F. 2006, A&A, 446, 813G.
- Gladysz, S. et al. 2008, PASP, 120, 1132
- Hillenbrand, Lynne A.; Strom, Stephen E.; Vrba, Frederick J.; Keene, Jocelyn 1992 Astrophysical Journal, vol. 397, no. 2, p. 613-643
- Hinz, P.M. et al. 2000, SPIE 4006, 349
- Hinz, Philip M.; Rodigas, Timothy J.; Kenworthy, Matthew A.; Sivanandam, Suresh; Heinze, Aren N.; Mamajek, Eric E.; Meyer, Michael R. 2010 The Astrophysical Journal, Volume 716, Issue 1, pp. 417-426
- Kenworthy et al. 2004, Advancements in Adaptive Optics. Edited by Domenico B. Calia, Brent L. Ellerbroek, and Roberto Ragazzoni. Proceedings of the SPIE, Volume 5490, pp. 351-358
- Kenworthy, Matthew A.; Mamajek, Eric E.; Hinz, Philip M.; Meyer, Michael R.; Heinze, Aren N.; Miller, Douglas L.; Sivanandam, Suresh; Freed, Melanie 2009 The Astrophysical Journal, Volume 697, Issue 2, pp. 1928-1933
- Kenworthy, Matthew A.; Codona, Johanan L.; Hinz, Philip M.; Angel, J. Roger P.; Heinze, Ari; Sivanandam, Suresh (2007) The Astrophysical Journal, Volume 660, Issue 1, pp. 762-769.
- Kopon et al. 2008 Proc. SPIE, Vol. 7015 p. 70156M-70156M-11
- Kopon et al. 2009 Proc. SPIE, Vol 7439, p74390
- Kopon, Derek; Close, Laird M.; Males, Jared; Gasho, Victor; Follette, Katherine 2010 Adaptive Optics Systems II. Edited by Ellerbroek, Brent L.; Hart, Michael; Hubin, Norbert; Wizinowich, Peter L. Proceedings of the SPIE, Volume 7736, pp. 77362V-11
- Law, N.M., et al. "Getting Lucky With Adaptive Optics: Fast Adaptive Optics Image Selection In The Visible With a Large Telescope." ApJ 692:924, (2009).
- Lenzen R., et al. 2005 proc "ESO workshop on science with AO", 115
- Lloyd-Hart 2000, PASP 112, 264
- Macintosh, B.A. et al. 2008 Wizinowich, Peter L. Proceedings of the SPIE, Volume 7015, pp. 701518-13
- Males, Jared R.; Close, Laird M.; Kopon, Derek; Gasho, Victor; Follette, Katherine, 2010 Adaptive Optics Systems II. Edited by Ellerbroek, Brent L.; Hart, Michael; Hubin, Norbert; Wizinowich, Peter L. Proceedings of the SPIE, Volume 7736, pp. 773660-13
- Park, Ryeojin; Close, Laird M.; Siegler, Nick; Nielsen, Eric L.; Stalcup, Thomas, 2006 PASP 118 159
- Potter 2003 Thesis (PhD). UNIVERSITY OF HAWAII, Source DAI-B 64/05, p. 2228, Nov 2003, 160 pages.

- Rigaut, Francois; Neichel, Benoit; Bec, Matthieu; Boccas, Maxime; Garcia-Rissmann, Aurea; Gratadour, Damien, 2010 1st AO4ELT conference - Adaptative Optics for Extremely Large Telescopes, held 22-26 June, 2009 in Paris, France. Edited by Y. Clénet, J.-M. Conan, Th. Fusco, and G. Rousset. EDP Sciences id.08001
- Racine, R. et al. "Speckle Noise and the Detection of Faint Companions". PASP, 111, 587 (1999).
- Roddier, F. 1999, Adaptive Optics in Astronomy, Cambridge Press.
- M. C. Roggemann & J. A. Meinhart. "Image Reconstruction By Means of Wave-Front Sensor Measurements in Close-Loop Adaptive-Optics Systems." JOSA, Vol 10, No. 9, 1996 (1993).
- Schaller, E. L., Brown, M. E., Roe, H. G., Bouchez, A. H., Trujillo, C. A. 2006, Icarus, 184, 517S.
- van der Plas, G., van den Ancker, M. E., Fedele, D., Acke, B., Dominik, C., Waters, L. B. F. M. & Bouwman, J. 2008, A&A, 485, 487V.
- Veran, J.P. et al. "Estimation of the Adaptive Optics Long-Exposure Point-Spread Function Using Control Loop Data." JOSA, Vol 14, No. 11, 3057 (1997).